On the Application of the Mixed Sensitivity Approach to a Real Control Problem Using Parametric and Nonparametric Models

MÁRCIO FANTINI MIRANDA[1] FÁBIO GONÇALVES JOTA[2]

[1]COLTEC - Technical School
Federal University of Minas Gerais
fantini@novell.cpdee.ufmg.br
[2]Electronics Eng. Dept.
Federal University of Minas Gerais
fabio@cpdee.ufmg.br
BRAZIL

Abstract: This paper considers the design and implementation of robust controllers for an Interacting Tank System (ITS) pilot-scale plant. The design aims at achieving good track-following performance for level and flow-rate control, despite changes in setpoint and/or operational conditions. It is presented a standard H_∞ design (mixed sensitivity) and two designs for the uncertain system: one for parametric uncertainties and the other for nonparametric uncertainties.

Key-Words: H_∞ Controller; μ-analysis; Mixed Sensitivity; Robust Control; Interacting Tanks

1 Introduction

The question of controlling *uncertain systems* has received considerable attention in the last ten years. Depending on the structure and type of the uncertainties present in the system, various frameworks have been considered, namely, robust H_∞ control (e.g. [4, 11, 14]), LMI (e.g. [5]), gain-scheduling (e.g. [10]), nonlinear H_∞ control (e.g. [13]). In the present work, we investigate a specific problem of robustness: the design of a controller capable of coping with uncertainties that appear on a real plant when the operating point varies around an equilibrium point (at which the corresponding linear system is calculated). In this case we have the so-called *parameter dependent system*. One way to deal with parameter-dependent systems for linearized models is within the standard H_∞ framework with norm-bounded uncertainties. For this, we find a nominal plant model and evaluate the effects of the perturbations. Depending on the uncertainty formulation chosen, either the standard H_∞ design [4] or the μ-synthesis [8] can then be used.

With an experimental motivation in mind, we implemented three different controllers for a plant which exhibits industrial characteristics. Questions about the uncertainty formulation, time response, choice of weighting functions (which specify the desired closed loop performance and stability margins), and the difference in performance among the controllers are investigated.

2 Notation and Preliminary Concepts

The notation adopted here is standard in the H_∞ framework. A family or a set of plants, $G(s)$, has its nominal value expressed as $G_0(s)$. The (suboptimal) H_∞ controller, $K(s)$ is the one that gives a closed loop matrix that satisfies:

$$||F_l(P_0, K)||_\infty \leq \gamma, \tag{1}$$

where $||.||_\infty$ is the H_∞ norm, F_l represents the lower FLT of P_o and K, and γ is some positive real number and $P_0(s)$ is the generalized matrix, which corresponds to G_0 plus the associated weighting matrices. Generally, the closed loop functions of interested is the *sensitivity function (or matrix)*, $S(s) = (I + G_0(s)K(s))^{-1}$ and the *complementary sensitivity function (or matrix)*, $T(s) = I - S(s)$.

The synthesis of the H_∞ controller can be accomplished from the so-called method of the *$S/KS/T$ mixed sensitivity problem* [2, 7, 11] where the generalized matrix is created from the nominal plant model, G_0, and from three weighting functions (or matrices). This is a standard H_∞ problem, whose objective is to find a $K(s)$ that satisfies:

$$\left\| \begin{array}{c} W_1(s)S(s) \\ W_2K(s)S(s) \\ W_3T(s) \end{array} \right\|_\infty \leq \gamma, \qquad (2)$$

where the W_i ($i = 1,2,3$) are the weighting functions associated with the error, the control signal and the plant output, respectively.

It is well known that, in the $S/KS/T$ problem, the resulting controller cancels the stable poles of the nominal plant [9]. In order to avoid this (undesirable) pole-zero cancelation, it is usuall to adopt a variation of the $S/KS/T$-scheme known as the GS/T-scheme [3, 12]. In this approach, two inputs, v and r, and two outputs, $z_1 = y$ and $z_2 = W_2u$, are considered (see figure 1). As in the $S/KS/T$-scheme, there are three weighting functions, W_r, W_v and W_2.

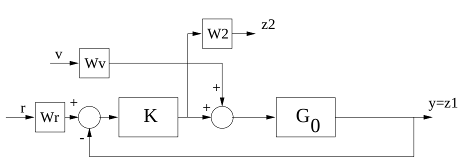

Figure 1: Block Diagram of the GS/T-sheme (standard).

For systems that are modeled as a “family” of plants representing the nominal plant plus an uncertainty block, the resulting problem is a *non-standard H_∞ problem* [11]. One way of representing the uncertainty is by means of the *nonparametric output multiplicative representation*, in which

$$G(s) = G_0(s)(I + \Delta(s)W_{od}(s)) \qquad (3)$$

where $\Delta(s)$ is any matrix such that $||\Delta||_\infty \leq 1$ and $W_{od}(s)$ is a diagonal matrix that represents the weights of the uncertainties as function of frequency. Other type of uncertainty representation is the *structured parametric representation* [14, 11]. For systems that can be expressed as $P(s) = F_u(P_0, \Delta)$, where F_u is the upper FLT and Δ is a matrix such that $||\Delta|| \leq \gamma$, the small gain theorem states that, if $||T_{zw}||_\infty \leq 1/\gamma$, then the closed loop system is stable for plants in the set $F_u(P, \Delta)$ [14].

2.1 Nonparametric Model Representation

The system we deal with can be represented by the following state space equations whose coeficients are functions of a parameter θ, which in turn depends on the the states $x(t)$ and the control signal, $u(t)$, that is, $\theta = f(x,u)$.

$$\begin{aligned} \dot{x} &= A(\theta)x + B(\theta)u \qquad (4) \\ y &= C(\theta)x + D(\theta)u. \qquad (5) \end{aligned}$$

The nominal model is defined for a specific $\theta = \theta_0$. θ_0 is the set of parameter values related to x_0 and u_0, i.e., the values of the states and control signal around which the linearization is done.

As we are interested in making the design in the frequency domain, we start by defining the 2×2 transfer matrix for the nominal system, i. e.,

$$G_0(s) = \left[\begin{array}{cc} g_0^{11}(s) & g_0^{12}(s) \\ g_0^{21}(s) & g_0^{22}(s) \end{array} \right]. \qquad (6)$$

We are looking for a family of plants given by the nonparametric (multiplicative) output uncertainty model, as given in equation (3).

A 2×2 uncertainty system is thus represented as:

$$\begin{aligned} y_1 &= g_0^{11}(1 + w_o^{11}(s)\Delta_1)u_1 + \qquad (7) \\ &\quad + g_0^{12}(1 + w_o^{12}(s)\Delta_2)u_2 \\ y_2 &= g_0^{21}(1 + w_o^{21}(s)\Delta_3)u_1 + \qquad (8) \\ &\quad + g_0^{12}(1 + w_o^{22}(s)\Delta_4)u_2. \end{aligned}$$

Since $|\Delta| \leq 1$, the maximum and minimum gain values of each (nominal) transfer function, $g^{ij}(s)$, are determined from the relations:

$$\begin{aligned} g^{ij}_{max} &= g^{ij}_0(1 + w^{ij}_o) \quad (9)\\ g^{ij}_{min} &= g^{ij}_0(1 - w^{ij}_o). \quad (10) \end{aligned}$$

On solving the system equations (9) and (10) for the functions w^{ij}, we get:

$$w^{ij}_o = \frac{g^{ij}_{max} - g^{ij}_{min}}{g^{ij}_{max} + g^{ij}_{min}}, \quad (11)$$

With the functions w^{ij}_o $(i, j = 1, 2)$ we define the matrix $W_o(s)$:

$$W_o(s) = \left[\begin{array}{cc} w^{11}_o(s) & w^{12}_o(s) \\ w^{21}_o(s) & w^{22}_o(s) \end{array} \right], \quad (12)$$

which will be diagonalized to define the model uncertainty as in (3).

3 The Interacting Tanks System

The experimental runs have been performed on a pilot-scale *Interacting Tank System*, ITS [6] (see figure 2). The ITS is composed of a $700l$ reservoir (TQ-01) and two $300l$ passively interconnected tanks (TQ-02 and TQ-03). The coupling between these two tanks can be manually controlled by means of flow valves FV-03 and FV-04. The basic operation of the system consists of pumping the liquid fluid from the reservoir (TQ-01) directly to the second tank (TQ-02). From TQ-02, the fluid flows naturally to the product tank (TQ-03). The liquid is then pumped back to the reservoir by BA-02. The simultaneous control of level and flow-rate in the third tank is accomplished by *equal-percentage* pneumatic valves, FCV-01 and FCV-02. So, there are two manipulated variables, u_1 and u_2, which are the control signals for the valves FCV-01 and FCV-02 (not the actual valve positions), and two outputs: y_1, the level, and y_2, the flow-rate at TQ-03 outlet. The ITS has been built with sensors and actuators as found in actual industrial plants. The data acquisition system also resembles real process control systems. A PLC is used to interface the plant to a microcomputer, where the control algorithms actually run. All the signal transmitions are accomplished via current loops of 4 to 20 mA.

3.1 System Modeling

The modeling of the ITS is based on the equations of the mass balance between the tanks. The model can be expressed by the system of equations:

$$\left\{ \begin{array}{lcl} \frac{dh_2}{dt} &=& \frac{q_i}{A} - \frac{q_{23}}{A} \\ \dot{h}_2 &=& \frac{f_1(u_1)}{AR_{hi}}\sqrt{h_1 + h_{b1} - h_c} - \frac{f_4(p)\sqrt{h_2 - h_3}}{A} \\ \frac{dh_3}{dt} &=& -\frac{q_o}{A} + \frac{q_{23}}{A} \\ \dot{h}_3 &=& -\frac{f_2(u_2)}{AR_{ho}}\sqrt{h_{b2} + h_3} + f_4(p)\frac{\sqrt{h_2 - h_3}}{A} \end{array} \right. \quad (13)$$

where q_i is the input flow-rate (in TQ-02), q_o is the output flow- rate (in TQ-03), q_{23} is the flow-rate between TQ-02 and TQ-03, h_2 is the level of TQ-02 and h_3 is the level of TQ-03. Both TQ-02 and TQ-03 have area A. The constant h_1 is the (average) level of tank TQ-01 and h_c corresponds to the height of the water column that exherts pressure on $BA01$ (see figure 2). h_{b1} and h_{b2} represent the pumping capacity of $BA01$ and $BA02$, respectively, expressed as heights of water column. The hydraulic resistances of the output and input are R_{ho} and R_{hi}, respectively. We consider h_2 as being the state x_1 and h_3 as being the state x_2. The functions $f_1(u_1)$ and $f_2(u_2)$ represent steady state characteristics of valves FCV-01 and FCV-02, respectively. The function $f_4(p)$ represents the relation between output flow-rate and the relative aperture of the manual valve FV-04. It is a constant value for a given valve aperture (for FV-04 fully open, $f_4(p) = 2.58$).

The linear model is given by:

$$\begin{aligned} \left[\begin{array}{c} \dot{x}_1 \\ \dot{x}_2 \end{array} \right] &= \left[\begin{array}{cc} -k_1 & k_1 \\ k_1 & -k_{12} \end{array} \right] \left[\begin{array}{c} x_1 \\ x_2 \end{array} \right] + \\ & \left[\begin{array}{cc} k_2 & 0 \\ 0 & k_3 \end{array} \right] \left[\begin{array}{c} u_1 \\ u_2 \end{array} \right] \quad (14) \\ \left[\begin{array}{c} y_1 \\ y_2 \end{array} \right] &= \left[\begin{array}{cc} 0 & 1 \\ 0 & t_1 \end{array} \right] \left[\begin{array}{c} x_1 \\ x_2 \end{array} \right] + \\ & \left[\begin{array}{cc} 0 & 0 \\ 0 & Ak_2 \end{array} \right] \left[\begin{array}{c} u_1 \\ u_2 \end{array} \right]. \quad (15) \end{aligned}$$

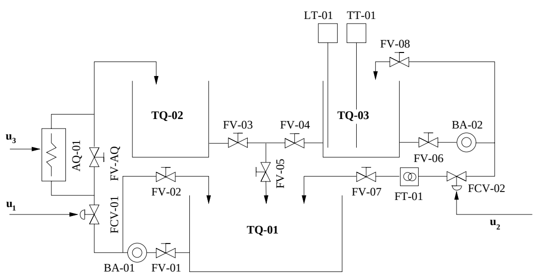

Figure 2: Schematic Diagram of the Interacting Tanks System, ITS

where the values of k_1, k_2 and k_3 vary with the chosen operating point and are given by:

$$k_1 = -\frac{f_4(p)}{2A\sqrt{x_{10}-x_{20}}} \quad (16)$$

$$k_2 = \frac{1}{A}\left.\frac{\partial f_1(u_{10})}{\partial u_1}\right| \sqrt{h_{10}+h_{b1}-h_c} \quad (17)$$

$$k_3 = -\frac{1}{A}\left.\frac{\partial f_2(u_{20})}{\partial u_2}\right| \sqrt{x_{20}+h_{b2}}. \quad (18)$$

$$k_4 = -\frac{1}{2}\frac{f_2(u_{20})}{R_{ho}}\frac{1}{\sqrt{x_{20}+h_{b2}}}. \quad (19)$$

$$k_{12} = k_1 - k_4. \quad (20)$$

$$t_1 = \frac{f_2(u_2)}{R_{ho}}\frac{1}{\sqrt{x_{20}+h_{b2}}}. \quad (21)$$

From the previuous state space model, we get the family of plants expressed as:

$$G(s) = \begin{bmatrix} \frac{-k_1k_2}{den} & \frac{k_3(s-k_1)}{den} \\ \frac{-k_1k_2t_1}{den} & \frac{k_3t_1(s-k_1)-Ak_3den}{den} \end{bmatrix}, \quad (22)$$

where,

$$den = s^2 - s(k_1+k_{12}) + k_1k_{12} - k_1^{12}.$$

The range of variations of the constants defined for the "family of plants" is given in the sequel.

3.2 Determination of the Operating Point and Related Constants

By considering the expected physical behavior of some plant variables and from previously gathered experimental data, we define the range of variations of the above constants. The nominal values are: $u_{10} = 0.455$, $u_{20} = 0.582$, $x_{10} = 0.510$, $x_{20} = 0.500$ and $f_4(100) = 2.58$. For the range of possible variations, we consider that the difference between the tanks TQ02 and TQ03 level varies from 5 to $10cm$, that is, $x_1 - x_2$ change in this interval. It has also been assumed that the control signals u_1 and u_2 vary, respectively, in the range of 0.2 to 1 and of 0 to 0.8. The average values of the water level in the three tanks have been taken as 50%; the range of variation of h_2 and h_3 being 0 to 1. With this configuration, the variation of the model coeficients are in the range:

$$\begin{array}{rll} -1.129\times10^{-2} & \le k_1 & \le -7.985\times10^{-3} \\ 3.20\times10^{-3} & \le k_2 & \le 6.12\times10^{-3} \\ -1.131\times10^{-2} & \le k_{12} & \le -7.995\times10^{-3} \\ 5.045\times10^{-4} & \le k_3 & \le 9.433\times10^{-4} \\ -2.216\times10^{-5} & \le k_4 & \le -9.984\times10^{-6} \\ 3.614\times10^{-7} & \le t_1 & \le 8.023\times10^{-7}. \end{array}$$

3.3 The Nonparametric Model for the ITS

As shown in equations (9) and (10), the values of the entries of W_o are functions of the g^{ij}_{max} and g^{ij}_{min}. Equation (11) gives the entries of $W_o(s)$ whose frequency responses are depicted in figure 3.

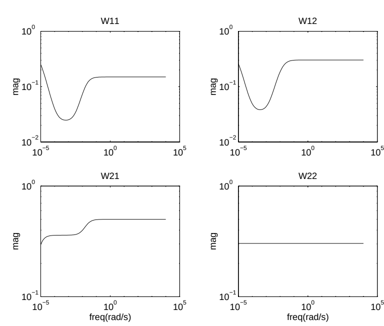

Figure 3: Frequency response of entries of $W_o(s)$

In order to represent the uncertainty system as in the equation (3), we define

$$W_{od} = \begin{bmatrix} w_o^{11} & 0 \\ 0 & w_o^{21} \end{bmatrix}. \quad (23)$$

that is, the entries of W_{od} are determined from the frequency response of W_o so as to encompass the worst-case dynamics (see figure 3).

3.4 The Parametric Model for the ITS

To derive the parametric model, it is only necessary to determine the range of the relevant parameter variation. The linear system is then represented by (7) and (8). The structured matrix Δ is composed of the previously defined uncertainties. Considering the range of variations of k_1,k_2,k_{12},k_3,k_4 and k_1 (given before), the final parametric uncertainty model results in:

$$G(s) = F_l(G_0(s), \Delta(s)), \qquad (24)$$

where $\Delta(s)$ is an 6×6 matrix such as $||\Delta||_\infty \leq 1$.

4 Problem Formulation

Our objetive is design three different controllers for the ITS plant and compare their performance, robustness properties and time responses. The implemented controllers are: *i)* a H_∞ controller designed by the mixed sensitivity approach (K_∞ controller); *ii)* a μ- controller for the parametric uncertainty model ($K_{\mu 1}$ controller), and *iii)* a μ-controller for the parametric uncertainty model ($K_{\mu 2}$ controller). In the first design, the K_∞ controller, we have used the standard GS/T-scheme (see figure 1). In the other two designs, $K_{\mu 1}$ and $K_{\mu 2}$ controllers, the configurations given in figures 4 and 5 have been respectively used.

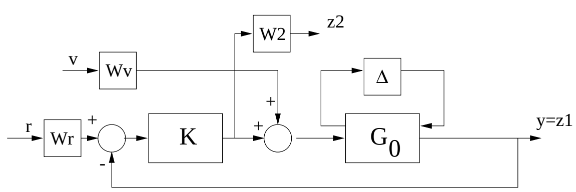

Figure 4: GS/T-scheme with parametric uncertainties using for the $K_{\mu 1}$ design.

5 Controller Design

Each design is based on the corresponding representation of the uncertainties and of the weighting functions. The matrices W_v, W_2 and W_r have been found after some trial-and-error procedure, using the rules given in [7] and [11]. In all cases, the design has been accomplished with the aid of μ-Analysis and Synthesis Toolbox [1] for Matlab. The generalized plant has been determined from the values for G_0, the chosen weighting functions and W_o. In the design of the K_∞ controller, the controller has been derived using the γ-interation [1, 11]. In the other two designs, we have made use of the $D-K$ iteration [1] which is a design that involves the γ-interation and the μ- analysis.

The resulting K_∞ controller has 8 states, i.e., the order of the generalized plant. After the D-K iteration, the $K_{\mu 1}$ controller has ended up with 20 states. The $K_{\mu 2}$ design, on the other hand, resulted in a controller with 14 states. Both $K_{\mu 1}$ and $K_{\mu 2}$ were reduced to a 5-state controller using a model reduction strategy [1], in order to simplify the computer implementation.

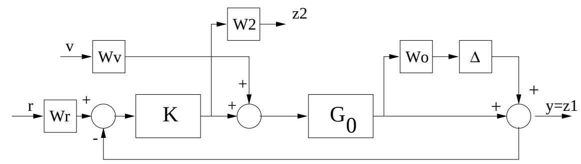

Figure 5: GS/T-scheme with nonparametric uncertainties using for the $K_{\mu 2}$ design

6 Robustness Analysis

Figures 6 and 7 show the robust analysis relative to controller $K_{\mu 1}$ and $K_{\mu 2}$, respectively. These figures show the shape of the μ over the frequency range.

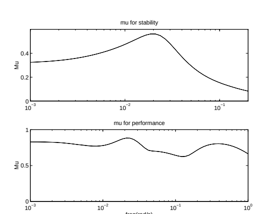

Figure 6: μ plot for robust stability and robust performance for the $K_{\mu 1}$ controller.

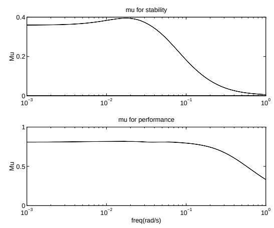

Figure 7: μ plot for robust stability and robust performance for the $K_{\mu 2}$ controller.

The results show that the adopted uncertainty formulation guarantees both robust stability and robust performance. This is so, because the μ-peak is always smaller than one.

7 Experimental Results

In this section, we present some results from experimental runs accomplished in the ITS pilot-scale plant. In the performed tests, variations on flow-rate and level have been purposedly imposed (at times $1000s$ and $4000s$).

Figure 8, 9 and 10 show the time response profile for tracking-following of the level loop for the three cases (since the flow-rate loop is relatively easy to control, we do not present them here).

7.1 Case 1: $K_\infty Controller$

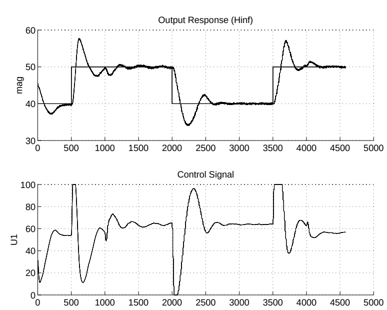

Figure 8: Time Response for the K_∞ controller

From figure 8 we can see that the reference tracking is achieved, but with some overshoot. The control signal does not present large and frequent variations, which can be considered a advantage from the valve wear point of view. This controller was not designed to have a robust response, and, as it will be seen, its control signal is smother than that of the μ-controllers.

7.2 Case 2: $K_{\mu 1}$ Controller

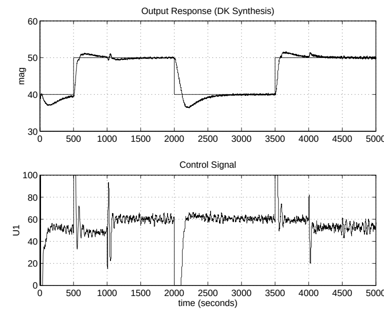

Figure 9: Time Response for the $K_{\mu 1}$ controller

The time response profile of $K_{\mu 1}$ controller, given in figure 9, can be considered as being very good, better than that of the previous one. It presents a faster controller with smaller overshoot. One problem with this controller is that the control signal oscilates with a frequency greater than the first controller, which results in a significant valve wear. The comparison of these two controllers emphasizes the required tradeoff between robustness and performance. It is interesting to note the perturbation occurring at $t = 1000s$, which is caused by a flow-rate variation.

7.3 Case 3: $K_{\mu 2}$ Controller

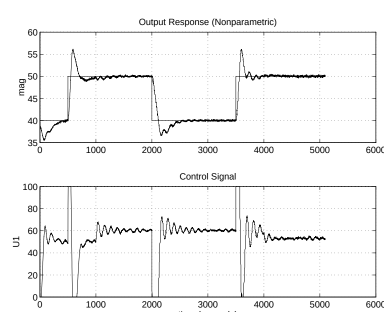

Figure 10: Time Response for $K_{\mu 2}$ controller

The performance of the third controller, given in figure 10, can be considered as being in the middle point between the first two. It presents a signal with more variations than that of the first controller and less than that of the second one. Its time response is similar to the one of the first case, with some improvements on the settling time.

8 Conclusions

The objectives of this work were the implementation of a robust control in a real plant and the investigation of the relevant issues that arise when we work with uncertainties systems. We have studied an uncertainty system where we compare the parametric model with the nonparametric one. While the robustness analysis of both $K_{\mu 1}$ and $K_{\mu 2}$ show that they are almost the same, the real time response indicate that they have important dynamic characteristic diferences, such as, frequent oscilators, overshoot and settling time, for example.

This work opens a wide range of possibilities for study related to the H_∞ design, such as, the choice of the order of the controller and the problem of uncertainty representations, all of them motivated by real control problems.

References

[1] G. J. Balas, J. C. Doyle, K. Glover, A. Packard, and R. Smith, *μ-Analysis and Synthesis Toolbox - User's Guide*, The MathWorks Inc., 1992.

[2] R. Y. Chiang, M. G. Safonov, and J. A. Tekawy, *h^∞ flight control design with large parametric robustness*, in American Control Conference (San Diego, CA), IEEE, 1990, pp. 2496–2501.

[3] U. Christen, *Engineering Aspects of H_∞ Control*, PhD thesis, Swiss Federal Institute of Technology, Zurich, Swiss, June 1996.

[4] J. C. Doyle, K. Glover, P. P. Khargonekar, and B. A. Francis, *State space solutions to standard h_2 and h_∞ control problems*, IEEE Trans. Aut. Control, 34 (1989), pp. 831–847.

[5] P. Gahinet, *Explict controller formulas fo lmi-based h_∞ synthesis*, Automatica, 32 (1996), pp. 1007–1014.

[6] F. G. Jota, A. R. Braga, C. M. Polito, and R. T. Pena, *Development of an interacting tank system for the study of advanced process control strategies*, in 38th IEEE Midwest Symposium on Circuits and Systems, IEEE, ed., vol. 1, 1995, pp. 441–445.

[7] P. Lundstrom, S. Skogestad, and Z.-Q. Wang, *Performance weight selection for h_∞ and μ-control methods*, Trans. Inst. Meas. and Control, 13 (1991), p. 241.

[8] A. Packard and J. Doyle, *The complex structured singular value*, Automatica, 29 (1993), pp. 71–109.

[9] J. Sefton and K. Glover, *Pole/zero cancellations in the general h_∞ problem with reference a two block design*, System and Control Letters, 14 (1990), pp. 295–306.

[10] J. S. Shamma and M. Athans, *Gain scheduling: Potential hazards and possible remedies*, IEEE Control Systems, 12 (1992), pp. 101–107.

[11] S. Skogestad and I. Postlethwaite, *Multivariable Feedback Control - Analysis and Design*, John Wiley and Sons, 1996.

[12] M. Steinbuch, P. J. M. van Gross, G. Schootstra, P. M. R. Wortelboer, and O. H. Bosgra, *μ synthesis for a compact disc player*, International Journal of Robust and Nonlinear Control, 8 (1998), pp. 168–189.

[13] A. J. van der Schaft, *l_2-gain analysis for nonlinear systems and nonlinear state feedback h_∞ control*, IEEE Trans. on Aut. Control, 37 (1992), pp. 770–794.

[14] K. Zhou, J. Doyle, and K. Glover, *Robust and Optimal Control*, Prentice Hall, 1996.